Synthesis of Hyperbranched Organo-Montmorillonite and Its Application into High-Temperature Vulcanizated Silicone Rubber Systems

Jincheng Wang, Yuehui Chen, Jihu Wang

College of Chemistry and Chemical Engineering, Shanghai University of Engineering Science, Shanghai 201620, People's Republic of China

Received 30 October 2007; accepted 10 April 2008
DOI 10.1002/app.29112
Published online 13 October 2008 in Wiley InterScience (www.interscience.wiley.com).

ABSTRACT: *N*,*N*-Di(2-hydroxyethyl)-*N*-dodecyl-*N*-methyl ammonium chloride was used as intercalation agent to treat Na^+-montmorillonite and form a type of organic montmorillonite (OMMT). Hyperbranched OMMT (HOMMT) was prepared by condensation reaction between OMMT and the monomer we synthesized. It was then used in the preparation of high-temperature vulcanizated silicone rubber (HTV-SR)/HOMMT nanocomposite. Different types of HTV-SR/HOMMT nanocomposites were prepared with different amounts of HOMMT and compared with the composites directly incorporated with OMMT. Tensile properties such as tensile strength, elongation at break, permanent distortion, and shore A hardness were researched and compared. A combination of Fourier transform infrared spectroscopy, wide angle X-ray diffraction, and transmission electron microscopy studies showed that HTV-SR/HOMMT composites were on the nanometer scale, and the structure of HTV-SR was not interfered by the presence of HOMMT. Results showed that the tensile properties of HTV-SR/HOMMT systems were better than that of the HTV-SR/HOMMT and HTV-SR. This was probably due to the surface effect of the exfoliated silicate layers and anchor effect of HOMMT in the SR matrix.
© 2008 Wiley Periodicals, Inc. J Appl Polym Sci 111: 658–667, 2009

Key words: hyperbranched organic montmorillonite; high-temperature vulcanizated silicone rubber; nanocomposites; characterization; mechanism

INTRODUCTION

The reinforcement of rubbers is expressed by the enhancement of tensile strength, modulus, and abrasion resistance of the vulcanizates. The main aim for filler addition is to improve certain properties and cheapen the compound.[1] Among several fillers, aerosilica is the most important reinforcing agent used in silicone rubber (SR) industry. Because of its high price, easy conglomeration, and harm to workers' health, researchers focused on the development of other reinforcing fillers such as clay, SiO_2, and TiO_2 as reinforcement materials for host polymers. Among these inorganic materials, clay has been receiving special attention in the field of nanocomposites because of its submicroparticle size and intercalation properties. Nanocomposites containing intercalated clay particles exhibit improved moduli, decreased gas permeability, and enhanced heat resistance, which makes clay a useful filler in polymeric composites.[2–12]

Only a few papers focused on the application of clay in SR matrix. Wang et al.[13] investigated the mechanical properties and thermal stability of SR/organic montmorillonite (OMMT) hybrids synthesized by means of solution intercalation. Results showed that the physical and mechanical properties of SR system with 1-phr OMMT were nearly equal to that of the SR with 3-phr aerosilica because of the exfoliation of OMMT and the resultant surface effect in the system. Zhou et al.[14] synthesized a novel exfoliated SR clay nanocomposite by hydroxyl-terminated polydimethylsiloxane and organic clay. The mechanical properties of the nanocomposites prepared by different intercalation agents were compared and also the reinforcing and intercalation mechanism were discussed. Zheng et al.[15] reported the polymerization of SR/MMT composites using octamethyl cyclotetrasiloxane and MMT as raw materials via monomer intercalation ring-opening polymerization. Results indicated that MMT had inhibition effect on the anion ring-opening polymerization and also was found to be an ideal initiator in cationic polymerization.

Typically, MMT, one of the layered clay minerals, is a hydrated alumina-silicate clay composed of

Correspondence to: J. Wang (wjc406@263.net).
Contract grant sponsor: Shanghai Educational Commission Common Project; contract grant number: 06NZ006.
Contract grant sponsor: Shanghai Leading Academic Discipline Project; contract grant number: p1402.
Contract grant sponsor: National Natural Science Funds; contract grant number: 50803034.

© 2008 Wiley Periodicals, Inc.

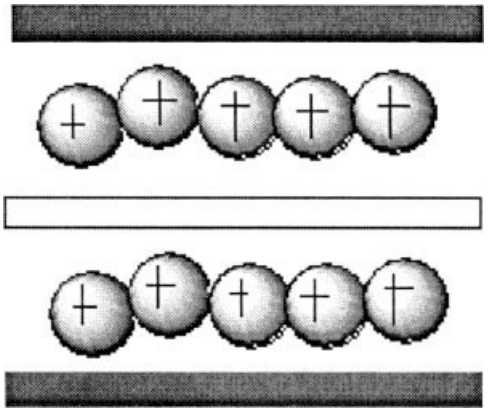

Figure 1 Scheme of the structure of MMT.

units of two silicate tetrahedral sheets with a certain alumina octahedral sheet. The silicate layers of MMT are planar, stiff and about 10 Å in thickness, 1000 to 2000 Å in length and width, and do not occur as isolated individual units but aggregate to form crystalline structures.[4] The scheme of the MMT structure is shown in Figure 1. For the efficient improvement of the properties of polymer-MMT composites, the basal spacing of MMT should be made accessible to the polymer chains; this may be realized through cation exchange between MMT and organic ammonium salts, which yields OMMT. However, the efficiency of OMMT in improving the properties of polymer materials depends not only on the surface nature of the OMMT but also on the state of the polymer materials. The high-temperature vulcanizated silicone rubber (HTV-SR) is a kind of solid state material, and it is operated at room temperature in the plasticator during production, which is not beneficial for its molecular chain to insert into the silicate layers and also is not beneficial for the silicate layers to disperse in the polymer matrix in nanometer degree.

To overcome these problems, hyperbranched modification technology is used in the preparation of exfoliated OMMT. Synthesis and application of hyperbranched macromolecules has received more attention because of their special structure. Hyperbranched macromolecules have porous and three-dimensional structure and plenty of functional end groups. This can make them more reactive. For high degree of branched structure, they are difficult to crystallize and have higher compatibility with other polymers.[16] In addition, the heat produced by the reactions between OMMT and the hyperbranched molecules can make the silicate layers easily exfoliated. Exfoliated OMMT can thus be obtained.

In this way, this hyperbranched OMMT (HOMMT) can be directly added into HTV-SR. Also, properties such as tensile strength, elongation at break, permanent distortion, and shore A hardness were researched and compared. Then, a combination of Fourier transform infrared spectroscopy (FTIR), wide angle X-ray diffraction (WAXD), and transmission electron microscopy (TEM) studies showed that HTV-SR/HOMMT composites were on the nanometer scale. Results showed that the use of HOMMT can greatly improve the physical and mechanical properties due to surface effect of silicate layers and "anchor" effect of HOMMT in the system.

EXPERIMENTAL

Materials

Na^+-MMT, industrial grade, was obtained from Zhejiang Fenghong Clay Company (Shanghai, China). *N*,*N*-Di(2-hydroxyethyl)-*N*-dodecyl-*N*-methyl ammonium chloride, chemically pure, was received from Zhejiang Chemical Agent Company (Hangzhou, China). Methyl acrylate, diethanolamine, methanol, and toluene-*p*-sulfonic acid were supplied by Shanghai Guoyao Chemical Company (Shanghai, China). HTV-SR, two components (Component A: gum with 40 wt % aerosilica, Component B: 2,4-terbutyl hexane peroxide), was supplied by Shanghai Huitian New Materials Company (Shanghai, China).

Preparation of OMMT

A 500-mL round-bottomed three-necked flask with a mechanical stirrer, thermometer, and condenser with drying tube was used as a reactor. Ten grams of MMT was gradually added to a prior prepared solution of *N*,*N*-di(2-hydroxyethyl)-*N*-dodecyl-*N*-methyl ammonium chloride (3.52 g), which was dissolved from 120 mL of ethanol and water mixture (weight ratio, 1 : 1), and the resultant suspension was vigorously stirred for 2 h. The treated MMT was repeatedly washed by deionized water. The filtrate was titrated with 0.1*N* of $AgNO_3$ until no precipitate of AgCl was formed to ensure the complete removal of chloride ions. The filter cake was then placed in a vacuum oven at 80°C for 12 h for drying. The dried cake was ground to obtain the OMMTs.

Preparation of HOMMT

Synthesis of intermediate monomer

About 0.1 mol methyl acrylate, 0.1 mol diethanolamine, and 10 mL methanol were added into a four-necked flask provided with a stirrer. The mixtures were treated at 35°C for about 4 h at N_2 atmosphere. The product was separated by filtration, washed until no methanol was remained. The product, *N*,*N*-dihydroxyl-3-aminmethyl propionate was obtained as stable transparent oil liquid. Yield: ~ 80%.

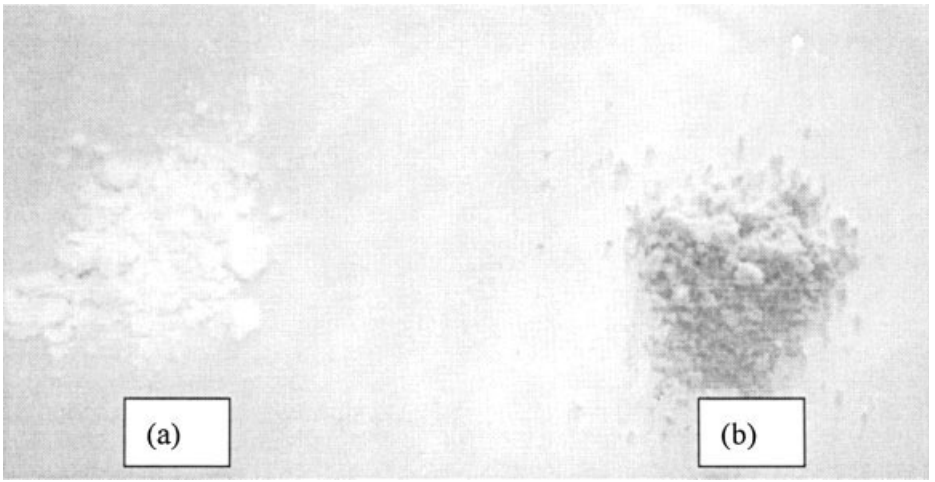

Figure 2 Photos of (a) OMMT and (b) HOMMT.

Synthesis of HOMMT

A 250-mL four-necked flask with a mechanical stirrer, thermometer, and a tube with N_2 atmosphere was used as a reactor. Ten grams of OMMT and 0.07 g of toluene-*p*-sulfonic acid (catalyst) were gradually added to 0.06 mol of a prior prepared solution of *N*,*N*-dihydroxyl-3-aminmethyl propionate. The resultant suspension was vigorously stirred for 10 h. The treated OMMT was repeatedly washed. The filter cake was then placed in a vacuum oven at 80°C for 6 h for drying. The dried cake was ground to obtain the HOMMTs.

Preparation of HTV-SR/HOMMT nanocomposites

Different amount of HOMMT or OMMT (1, 2, 3, 4, 5 phr) were added into the HTV-SR systems with 40 wt % aerosilica on a double roller plasticator. After mixing for 20 min, 0.8 g of 2,4-terbutyl hexane peroxide was added, and different types of HTV-SR composites were prepared. Then, the mixture was molded in a dumbbell mold. Curing was conducted at room temperature and at 175°C for 5 min, after which an elastic film was obtained.

Characterization

The photos of OMMT and HOMMT were taken by a digital Sony camera. Infrared transmission spectra of MMT, OMMT, HOMMT, HTV-SR/HOMMT, and HTV-SR/OMMT composites were obtained using a FTIR spectrometer, model Dos X from Nicolet. The scan range was from 4000 to 700 cm^{-1} with a resolution of 2 cm^{-1}.

To measure the change of gallery distance of OMMT, HOMMT, HTV-SR/OMMT, and HTV-SR/HOMMT before and after intercalation, WAXD was performed at room temperature with a Rigaku D-Max/400 (Japan) X-ray diffractometer. The X-ray beam was nickel-filtrated Cu Kα (λ = 0.154 nm) radiation operated at 50 kV and 150 mA. X-ray diffraction data were obtained from 1 to 10° (2θ) at a rate of 2°/min.

The tensile properties of the vulcanizates were measured with dumbbell specimens (6-mm wide in cross section) according to the Chinese National Standard GB 528-82. The value for each sample was taken as the median value of five specimens. These tests were carried out at room temperature on an universal tensile testing machine (XL-250A, Guangzhou, China) with a crosshead speed of 500 mm/min. The tensile specimens for each composition were tested, and the stress and strain at break were determined. Hardness measurements were performed according to GB 531-83 on a Shore A hardness tester.

The samples for TEM were first prepared by microtoming the composites into 80- to 100-nm-thick slices at −90°C. The graphs were obtained with H-800 instrument using an acceleration voltage of 200 kV.

RESULTS AND DISCUSSION

Analysis of OMMT and HOMMT

Figure 2 shows the photos of OMMT and HOMMT which we synthesized. It can be seen that OMMT is a kind of pale yellow powder, which can be easily dispersed. However, the HOMMT exhibits a dark gray color. It has some characteristics of polymeric materials.

Analysis of OMMT

The FTIR spectra of original MMT and OMMT are shown in Figure 3. The stretching vibration of —OH

group appeared between 3620 and 3650 cm^{-1}. This is attributed to the physical and chemical water existing in the Na^+-MMT. The peaks at 1030 and 700 cm^{-1} resulted from the stretching vibration of Si—O and Al—O bonds in the MMT structure. In the spectra of OMMT, except for the peaks existing in the MMT, the presence of new peaks at 2800–3000 cm^{-1} and 1469 cm^{-1} is shown, which were caused by C—H stretching and bending absorptions in the organic intercalation agent. The disappearing peaks at 1640 cm^{-1} (belongs to bending vibrations of O—H) illustrated the disappearance of inorganic water that exists in the silicate layers in MMT. This environment is beneficial for the exchanging of Na^+ cations in the MMT and $-\overset{|}{\underset{|}{\overset{+}{N}}}-$ cations in the intercalation agents.[17,18]

The WAXD patterns of original MMT and OMMT are shown in Figure 4. Curve (a), WAXD of pure MMT, shows a characteristic peak at 6° of 2θ, which was assigned to the 001 basal reflection. In Curve (b), there were three peaks in the WAXD spectrum. This indicated the different expansion degree of silicate layers in the OMMT. The research on the organic modification of MMT indicates that only one peak exist in the OMMT, which was modified by common intercalation agent, such as octadecyl trimethyl ammonium chloride or dodecyl amine.[19] The special structure of this OMMT may be caused by the special structure of the intercalation agent, *N*,*N*-di(2-hydroxyethyl)-*N*-dodecyl-*N*-methyl ammonium chloride. The underlying mechanism may be related to the strong polarity of —OH groups, branching chains of dihydroxethyl, and space-distributing morphology of molecular chains of this intercalation agent.

The MMT clay is a phyllosilicate mineral. Cations such as Na^+, K^+, and Ca^{2+} compensate the negative charge that exists in the crystal lattice of the each silicate layer in MMT. Polar molecules such as *N*,*N*-di(2-hydroxyethyl)-*N*-dodecyl-*N*-methyl ammonium chloride, which can make MMT more organophilic, can penetrate between the layers and swell. The schematic depicting the intercalation process between original MMT and the intercalation agent is illustrated in Figure 5. The interlayer spacing of OMMT is so large (5.25 nm, calculated from Bragg formula: $2d \sin \theta = n\lambda$) that it is greater than the extended chain length of the intercalation agent.

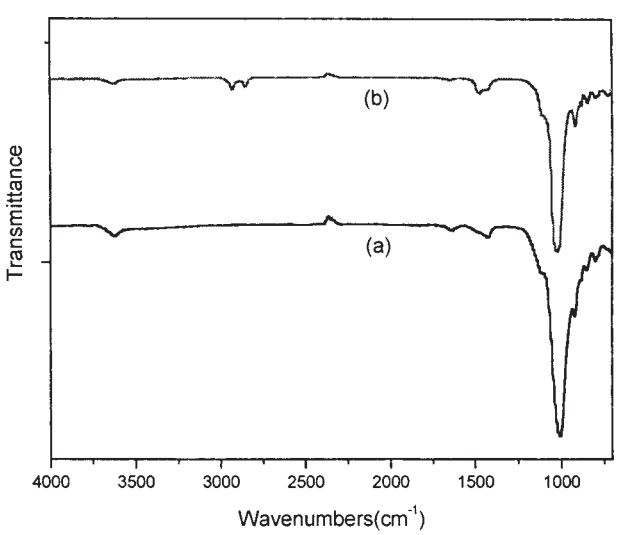

Figure 3 FTIR spectra of (a) MMT and (b) OMMT.

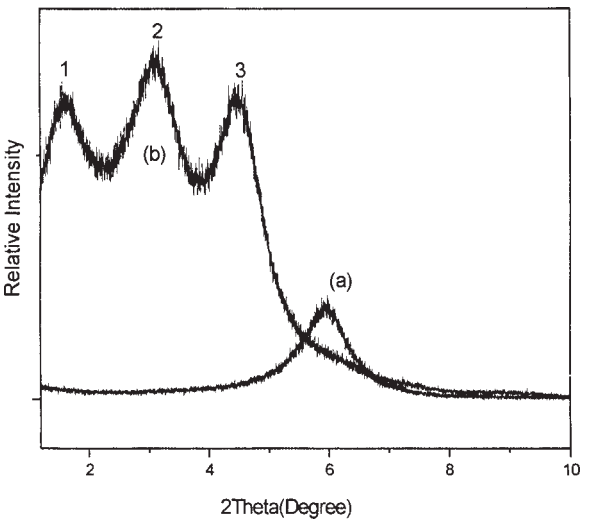

Figure 4 WAXD spectra of (a) MMT and (b_{1-3}) OMMT.

Analysis of HOMMT

The FTIR spectra of the monomer and HOMMT are shown in Figure 6. In the spectra of the monomer, the peaks between 3250 and 3650 cm^{-1} were caused by the stretching of the two hydroxyl groups and the peaks between 2800 and 3000 cm^{-1} resulted from the stretching vibration of C—H bond. The appearance of strong peaks at 1760 and 1100 cm^{-1} is attributed to the —C=O and —C—O— bonds in $-CH_2CH_2COOCH_3$. The hydrogen in —NH— is very active. It can destroy the double bonds in methyl acrylate. This addition reaction may result in the development of C—N bonds and thus lead to the appearing of peaks at 1270 cm^{-1}.

In the spectra of HOMMT, except for the peaks of OMMT, the presence of new peaks at 1275, 1280–1450, 2800–3000, and 3250–3650 cm^{-1} is shown, which were caused by corresponding stretching and bending absorptions in the monomer. The peaks at 1760 cm^{-1} disappeared and this illustrated the condensation reactions between $-OCH_3$ in the monomer and —OH in OMMT.

The WAXD spectra of HOMMT are shown in Figure 7. Compared with OMMT, no obvious peaks were observed in Curve (b), which was ascribed to

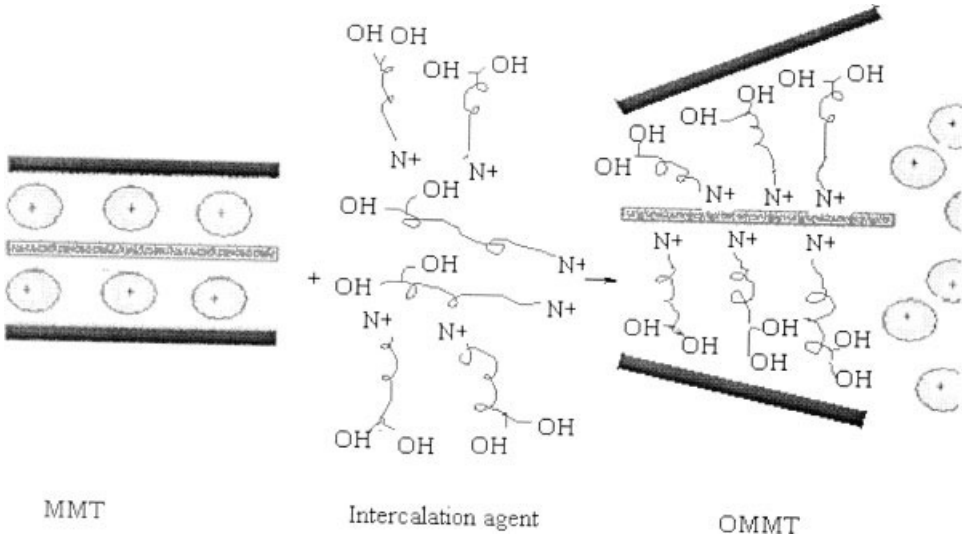

Figure 5 Scheme of intercalation process of MMT.

the exfoliated microstructure of HOMMT. The exfoliation may be caused by the energy produced from condensation reaction between OMMT and the monomer.

The reaction of synthesis of monomer is shown in Figure 8. It belongs to the Michael additional reaction. The H atom in —NH— of diethanolamine is very reactive and it can react with C=C in methyl acrylate to produce $^{-N-}_{|}$. The methanol used here is a kind of solvent and phase transfer agent. It can accelerate the dissolution of the two reactors and improve their reaction rate. The schematic depicting the reaction process between HOMMT and the monomer is illustrated in Figure 9. In this reaction, a condensation reaction occurs between —OCH_3 in the monomer and —OH in OMMT. Because of the interactions and the corresponding heat produced between silicate layers and hyperbranched molecules, a nanotype of OMMT can be obtained.

Analysis of HTV-SR composites

Tensile properties

Figures 10–13 show the tensile properties such as tensile strength, elongation at break, permanent distortion, and shore A hardness of HTV-SR/HOMMT and HTV-SR/OMMT composites.

The tensile strength of HTV-SR addition of 1-phr HOMMT (HTV-SR/HOMMT-1) was 10.7 MPa. It was improved almost 30% compared with that of HTV-SR. The elongation at break of HTV-SR/HOMMT composites also showed a remarkable enhancement. It was improved from 300 to 500%, 1.67 times compared with that of HTV-SR. This is

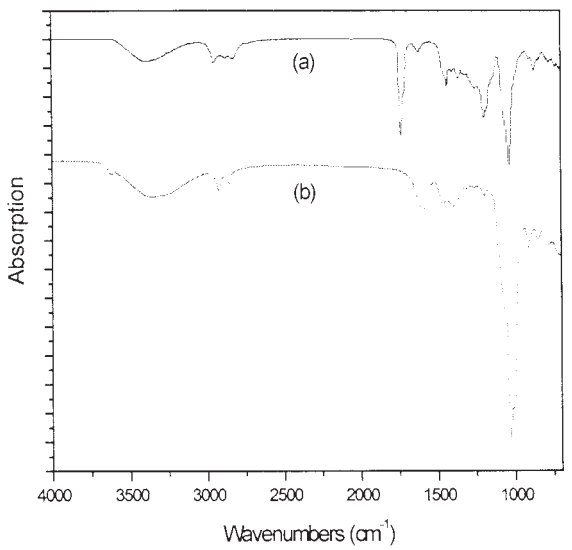

Figure 6 FTIR spectra of (a) monomer and (b) HOMMT.

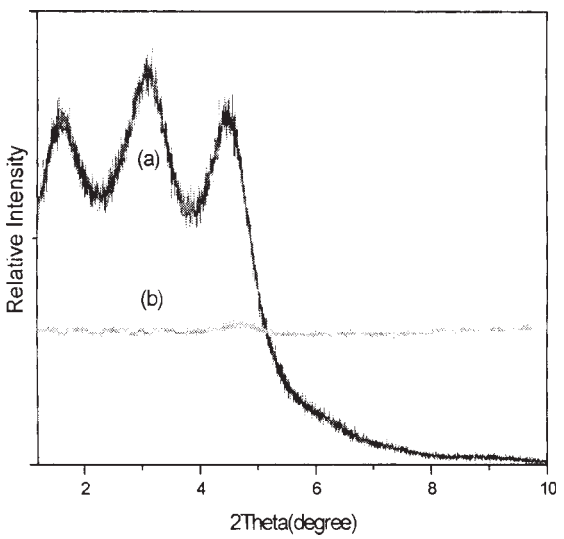

Figure 7 WAXD spectra of (a) OMMT and (b) HOMMT.

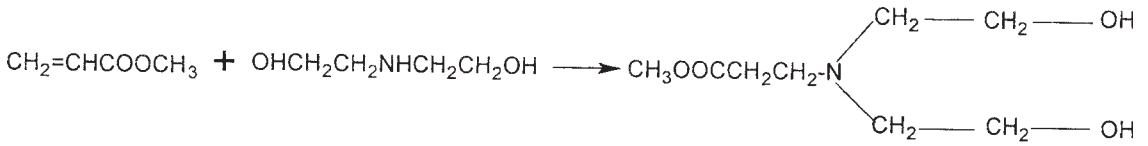

Figure 8 Chemical reaction between methyl acrylate and diethanolamine.

probably due to the silicate layers in the system. With the increasing content of HOMMT, the tensile strength decreased. This may be caused by the agglomeration of HOMMT in this composite. However, the addition of HOMMT can increase the permanent distortion and decrease the hardness of HTV-SR. The HOMMT, in some extent, may decrease the crosslinking density.

In the composite filled with different content of OMMT, the tensile strength and elongation at break showed a little decrease, and the permanent distortion showed a slight increase. This is attributed to the nonintercalated or exfoliated state of OMMT in the composites. An increase of hardness may be attributed to the special characteristic of OMMT.[20]

Microstructure analysis

WAXD analysis

An important measure of the degree of silicate dispersion and exfoliation in HTV-SR can be obtained by WAXD measurements. A series of WAXD patterns of composites containing 1 phr of HOMMT and OMMT are shown in Figure 14. No obvious peaks were observed in Figure 14(a), which was due to the original microstructure nature of HTV-SR. When 1 phr of HOMMT was incorporated, no obvious peaks were observed due to the loss of structure registry, indicating the possibility of having exfoliated silicate layers dispersed in the polymer matrix. The peaks appearing at $2\theta = 3.0^\circ$ and 4.7°, which had something to do with the original silicate layer space of OMMT [shown in Fig. 9(b)], illustrated the existence of stacked OMMT of crystallographic order in the composites.[21–23]

TEM analysis

Further evidence of dispersion of silicate layers in the case of HTV-SR/HOMMT-1 and HTV-SR/OMMT-1 composite was supported by TEM photomicrographs, as shown in Figure 15. From Figure 15(a), it can be observed that most silicate layers were dispersed homogeneously into the matrix.[24] The dark zones are the cross sections of the silicate layers. These silicate layers are surrounded by hyperbranched polymers and thus cannot be seen much clearly. As can be known from other references,[23] the thickness of the silicate layers of OMMT (dark lines) was about 1 nm. The distance between most of the silicate layers of OMMT in the SR matrix ranged from 10 to 20 nm, which are far larger than the original silicate layer spacing of 1.9–5.2 nm. This is evidence that these organoclays were mostly exfoliated in the matrix. From Figure 15(b), more clusters or agglomerated particles were detected, and the not intercalated or exfoliated structure in the system resulted in the lower tensile properties of the composite.

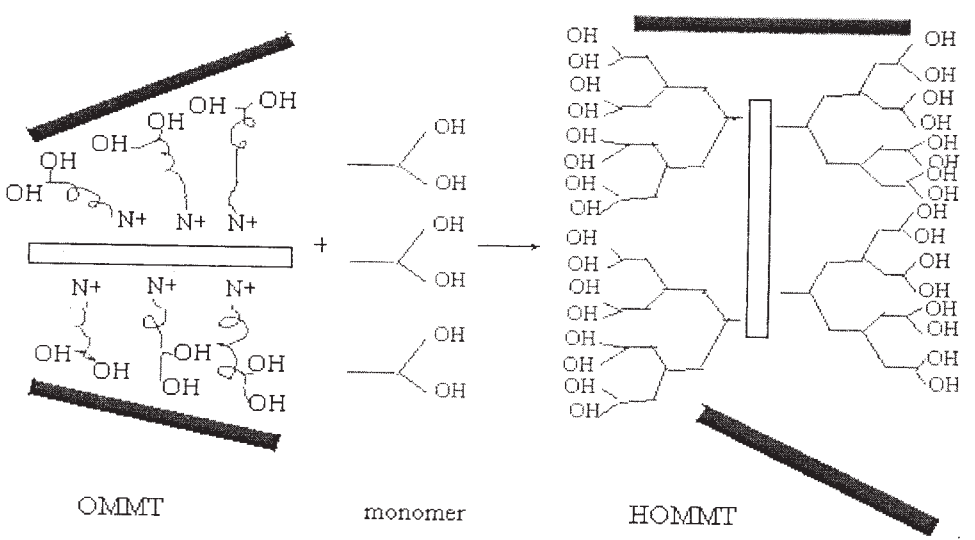

Figure 9 Scheme of hyperbranched reactions between OMMT and the monomer.

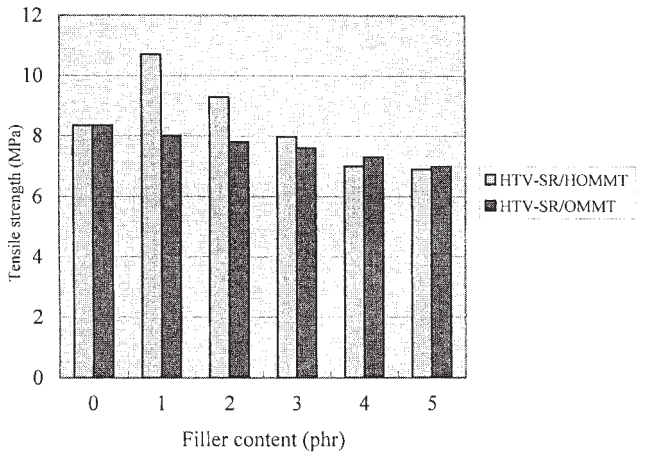

Figure 10 Tensile strength of HOMMT- and OMMT-filled HTV-SR composites.

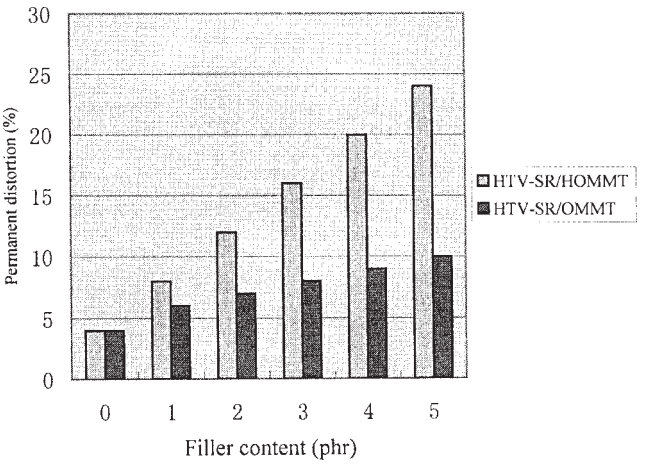

Figure 12 Permanent distortion of HOMMT- and OMMT-filled HTV-SR composites.

FTIR analysis

The microdomain structure of HTV-SR, HOMMT- and OMMT-filled HTV-SR composites were analyzed by FTIR as shown in Figure 16. It was found that the positions of peaks for distinctive functional groups were identical both in pure HTV-SR, HTV-SR/HOMMT-1, and HTV-SR/OMMT-1 composites, which means that the segmented structure of HTV-SR had not been affected much by the presence of HOMMT and OMMT.[25]

Mechanism analysis

A rigorous thermodynamic treatment based on the lattice-based mean field theory by Vaia and Giannelis[26,27] indicates that nanostructure formation occurs if the free energy change per interlayer volume (ΔF_V) is negative. ΔF_V can be expressed as follows:

$$\Delta F_V = \Delta E_V - T\Delta S_V \tag{1}$$

where ΔE_V and ΔS_V are the enthalpy and entropy change per interlayer volume, respectively, and T is the temperature. Since small increases in the gallery spacing do not strongly affect the total entropy change, intercalation will rather be driven by the changes in total enthalpy,[28] which is expressed as follows:

$$\Delta E_V = \varphi_1\varphi_2\frac{1}{Q}\left(\frac{2}{h_0}\cdot(\varepsilon_{sp}-\varepsilon_{sa})+\frac{2}{r}\varepsilon_{ap}\right) \tag{2}$$

where φ_1 and φ_2 are interlayer volume fraction of intercalated polymer and tethered surfactant chains, Q is a constant near unity, h_0 is the initial gallery height of organoclay, and r is the radius of the intercalation surface of tethered surfactant chains. ε_{sp}, ε_{sa}, and ε_{ap} represent the intercalation energies per area between the layered silicate and the polymer, the layered silicate and the intercalation agent, and the intercalation agent and the polymer, respectively. In the case of HTV-SR/HOMMT-1 nanocomposite, the addition of HOMMT increased the polarity of the matrix. In this nanocomposite, the interactions

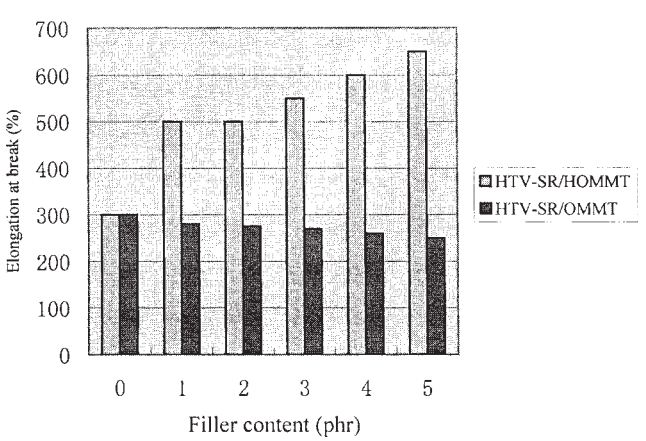

Figure 11 Elongation at break of HOMMT- and OMMT-filled HTV-SR composites.

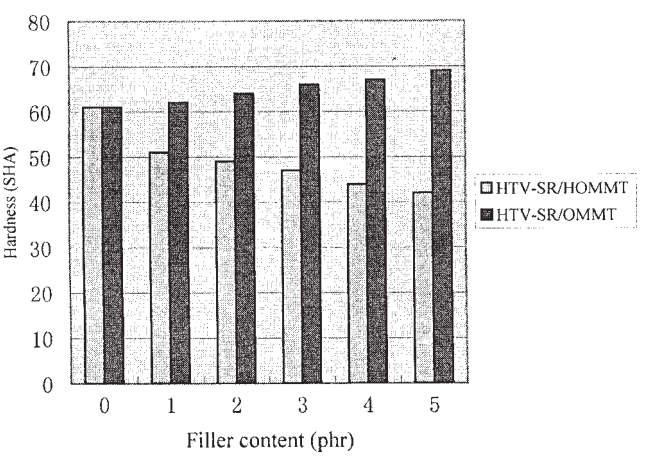

Figure 13 Shore A hardness of HOMMT- and OMMT-filled HTV-SR composites.

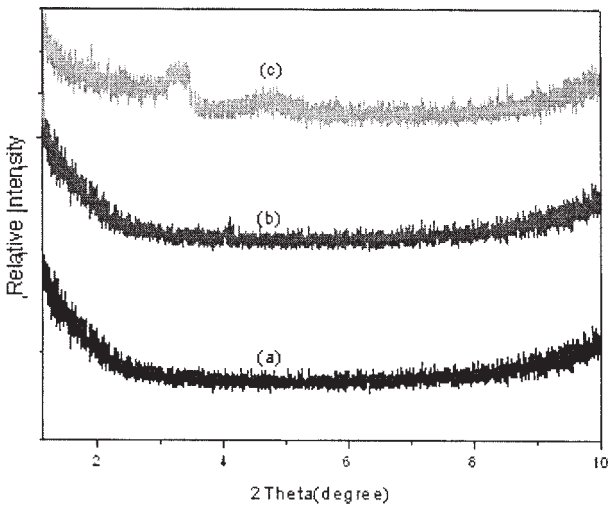

Figure 14 WAXD spectra of (a) HTV-SR; (b) HTV-SR/HOMMT-1; (c) HTV-SR/OMMT-1.

between the intercalation agent and the polymer, and the layered silicate and the polymer were also increased to the highest, leading to a most favorable ε_{ap} and ε_{sp}. So there is a favorable excess enthalpy to enhance the dispersion of the HOMMT, resulting in the formation of intercalated nanostructures. When the 1 phr of OMMT was directly incorporated into the SR system, the interactions between intercalation agent and the polymer, and the layered silicate and the polymer were decreased, which results in a decreased ε_{ap} and ε_{sp}, and a decrease of the enthalpy, which can decrease the dispersion degree of the OMMT.

The increase in the tensile strength and elongation at break of HTV-SR/HOMMT-1 can be attributed to the dispersion of the silicate layers in the crosslinking SR matrix. The different crack characteristics of HTV-SR, HTV-SR/HOMMT-1, and HTV-SR/OMMT-1 under tensile strength are depicted in Figure 17. The reason for the difference can be related to the parameters such as bound elastomer (continuous elastomer matrix restricted by silicate layers), elastomer shell creation (voids in the elastomer) in the vicinity of silicate layers, and the occlusion of elastomer within the clay galleries. Thus, an increase of tensile strength is expected when HOMMT was incorporated. The failure of the three specimens upon tensile strength starts with small cracks. If the elastomeric network is capable of dissipating the inputted energy (e.g., by converting into heat), then it can withstand higher stresses. In HTV-SR, numerous voids (subcritical cracks) appear during drawing

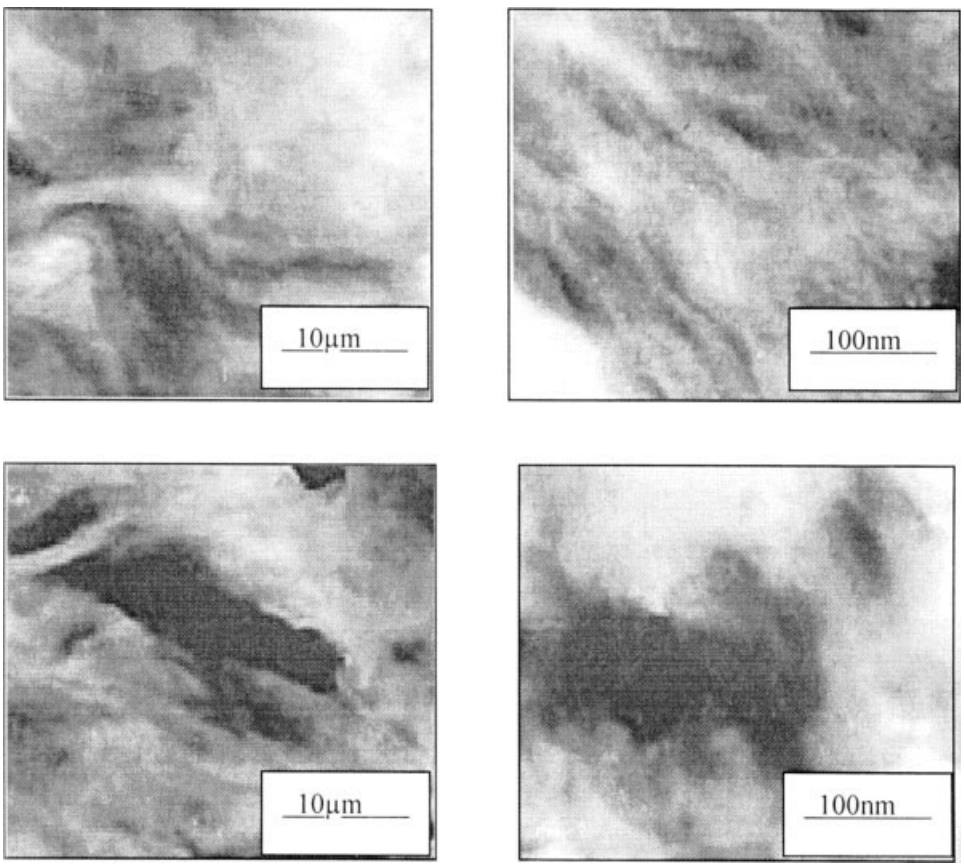

Figure 15 TEM photos of (a) HTV-SR/HOMMT-1 and (b) HTV-SR/OMMT-1.

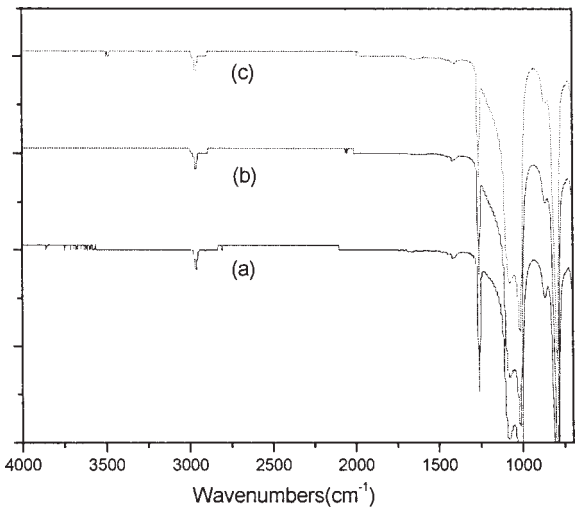

Figure 16 FTIR spectra of (a) HTV-SR; (b) HTV-SR/HOMMT-1; (c) HTV-SR/OMMT-1.

and cracks can be generated via voiding [shown in Fig. 17(a)]. The fracture mechanism of HTV-SR/HOMMT-1 is assumed to be platelet orientation, chain slippage, zig-zag energy dissipation. The surface effect of the silicate layers and the "anchor" reaction (shown in Fig. 18) between the functional group —OH in HOMMT and the molecular chains in HTV-SR can restrict the movement of polymer chains and combine them with silicate layers, which may reduce the amount and size of voids in their vicinity [shown in Fig. 17(b)]. The increase of the crack path around the silicate layers ("zig-zag" route) can also be considered as a mechanism of energy dissipation. By this suggested model, the increase in tensile properties seems to be as expected for this clay-reinforced nanocomposite. Furthermore, the decrease in the tensile properties with the direct addition of OMMT can be explained by the onset of large

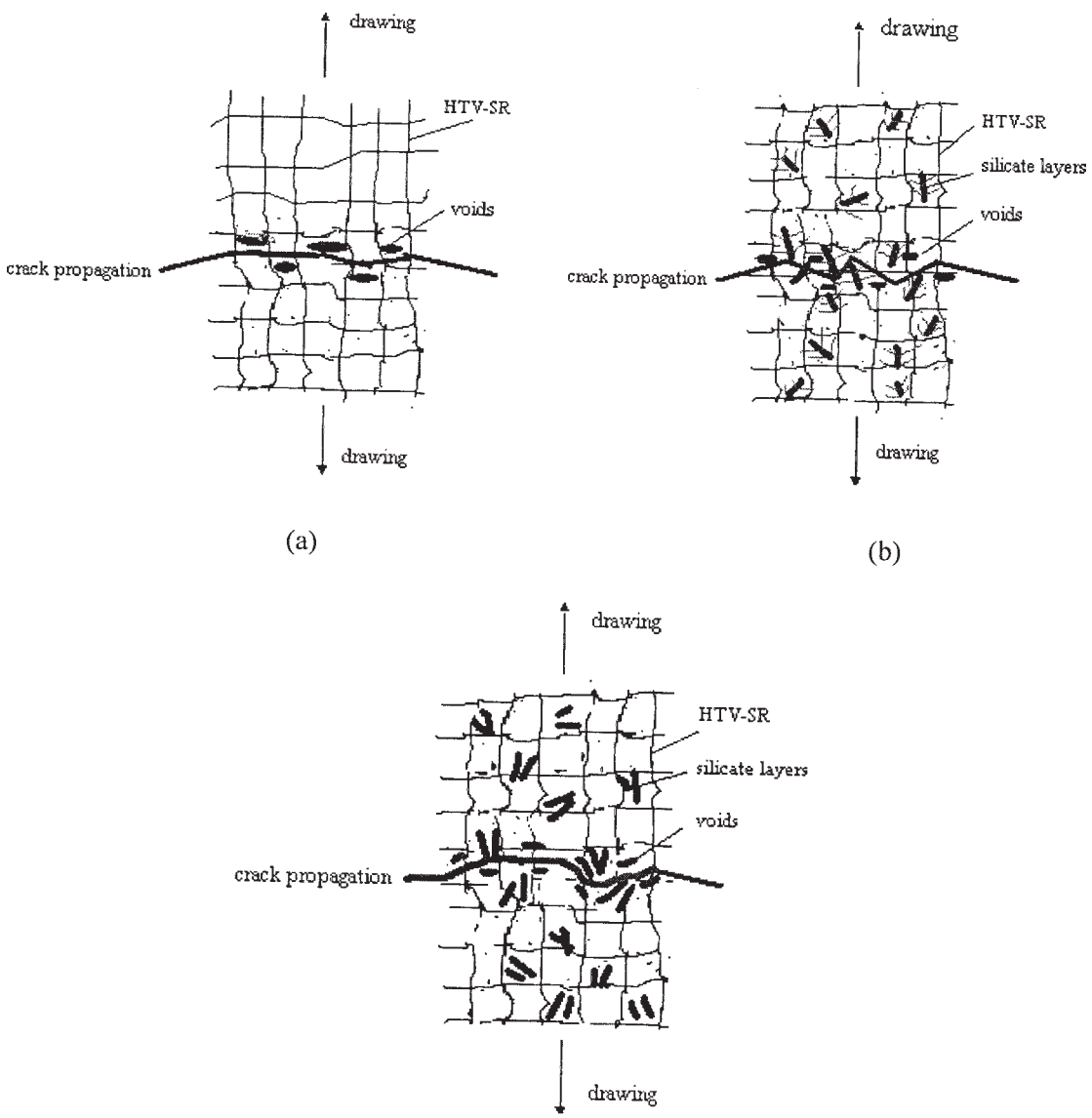

Figure 17 Scheme of failure development during tensile drawing: (a) HTV-SR; (b) HTV-SR/HOMMT-1; (c) HTV-SR/OMMT-1.

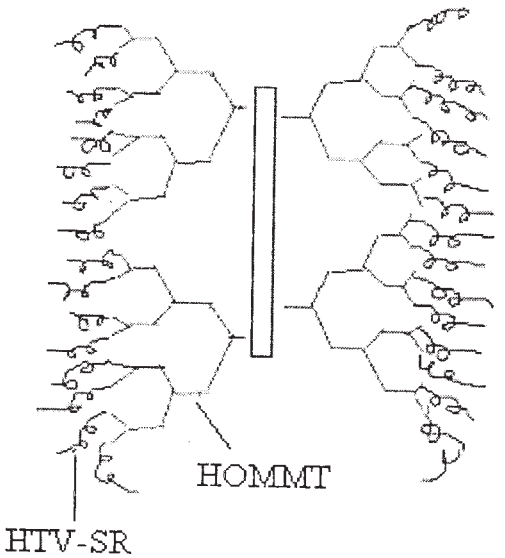

Figure 18 Scheme of anchor reaction exists in HTV-SR/HOMMT-1.

agglomerates, which may decrease the crack path around the silicate layers [shown in Fig. 17(c)] and favor the initiation of catastrophic failure.[29]

CONCLUSIONS

HOMMT was prepared by condensation reaction and was successfully applied into HTV-SR system. FTIR, WAXD, and TEM results verified the incorporation of this HOMMT into HTV-SR matrix and revealed that the degree of basal-spacing expansion was largely increased and an exfoliated nanocomposite was formed. The enhanced tensile properties demonstrated its efficiently reinforcing properties. Results showed that HTV-SR/HOMMT-1 nanocomposite had the best properties compared with that of HTV-SR/OMMT-1 composite because of the good dispersion of nanometer silicate layers and resultant "anchor" effect of the hyperbranched macromolecules in the composite.

References

1. Arroyo, M.; Lopez-Manchado, M. A.; Herrero, B. Polymer 2003, 44, 2447.
2. Vaia, R. A.; Jandt, K. D.; Kramer, E. J. Macromolecules 1995, 28, 8080.
3. Giannelis, E. P. Adv Mater 1996, 8, 29.
4. Alexandre, M.; Dubois, P. Mater Sci Eng R 2000, 28, 1.
5. Hachett, E.; Manias, E.; Giannelis, E. P. Chem Mater 2000, 12, 2161.
6. Bujdak, J.; Hachett, E. P.; Giannelis, E. P. Chem Mater 2000, 12, 2168.
7. Fu, X.; Qutubuddion, S. Polymer 2001, 42, 807.
8. Yoon, J. T.; Jo, W. H.; Lee, M. S. Polymer 2001, 42, 329.
9. Usuki, A.; Tukigase, A.; Kato, M. Polymer 2002, 43, 2185.
10. Wang, J. C.; Chen, Y. H.; Jin, Q. Q. J Adhes Sci Technol 2006, 20, 261.
11. Wang, J. C.; Chen, Y. H.; Jin, Q. Q. High Perform Polym 2006, 18, 325.
12. Lan, T.; Kaviratna, P. D.; Pinnavaia, T. J. Chem Mater 1995, 7, 2144.
13. Wang, J. C.; Chen, Y. H.; Jin, Q. Q. Macromol Chem Phys 2005, 206, 2512.
14. Zhou, N. L.; Xia, X. X.; Wang, Y. R. Acta Polym Sinica 2002, 2, 253.
15. Zheng, J. P.; Li, P.; Hao, W. L. J Tianjin Univ 2000, 33, 670.
16. Tan, H. M.; Luo, Y. J. Hyper-Branched Polymers; Chemical Industry Press: Beijing, 2005.
17. Ma, J.; Xu, J.; Ren, J. H. Polymer 2003, 44, 4619.
18. Wei, F.; Abdellatif, A. K.; Bernard, R. Macromol Rapid Commun 2002, 23, 705.
19. Tsutomu, T.; Yong, G. J Appl Polym Sci 2003, 90, 4075.
20. Younghoon, K.; James, L. W. J Appl Polym Sci 2003, 90, 1583.
21. Xu, R. J.; Manias, E.; Alan, J. S.; Runt, J. Macromolecules 2001, 34, 338.
22. Yao, K. J.; Song, M.; Hourston, D. J. Polymer 2002, 43, 1018.
23. Gatos, K. G.; Sawanis, N.; Apostolov, A. A.; Thomann, R.; Karger-Kocsis, J. Macromol Mater Eng 2004, 289, 1081.
24. Zhang, Z. J.; Zhang, L. N.; Yang, L. Polymer 2005, 46, 133.
25. Rodlert, M.; Christopher, G. P.; Garamszegi, L. Polymer 2004, 45, 952.
26. Vaia, R. A.; Giannelis, E. P. Macromolecules 1997, 30, 7990.
27. Vaia, R. A.; Giannelis, E. P. Macromolecules 1997, 30, 8000.
28. Manias, E.; Touny, L.; Wu, K.; Strawhecher, B. Chem Mater 2001, 13, 3516.
29. Mousa, A.; Karger-Kocsis, J. Macromol Mater Eng 2001, 286, 260.